

1 **The *Candida albicans* ζ -crystallin homolog Zta1 promotes resistance to oxidative stress**

2

3 Rafael M. Gandra¹, Chad J. Johnson², Jeniel E. Nett^{2,3}, and James B. Konopka^{1*}

4

5 ¹ Department of Microbiology and Immunology, Stony Brook University, Stony Brook, New York,
6 United States of America

7 ² University of Wisconsin-Madison, Department of Medicine

8 ³University of Wisconsin-Madison, Department of Medical Microbiology & Immunology

9 Corresponding Author:

10 * Corresponding author: james.konopka@stonybrook.edu

11

12

13

14 Running title: Zta1 promotes resistance to oxidative stress in *Candida albicans*

15

16 Keywords: *Candida albicans*, ζ -crystallin, Zta1, oxidative stress, quinone, quinone reductase,
17 flavodoxin like protein

18

19 Word count

20 Abstract: 189 words

21 Importance: 100 words

22 Text (excluding the references, table footnotes, and figure legends): 5,037

23

24 **ABSTRACT**

25 The fungal pathogen *Candida albicans* is capable of causing lethal infections in humans.
26 Its pathogenic potential is due in part to the ability to resist various stress conditions in the host,
27 including oxidative stress. Recent studies showed that a family of four flavodoxin-like proteins
28 (Pst1, Pst2, Pst3, Ycp4) that function as quinone reductases promotes resistance to oxidation
29 and is needed for virulence. Therefore, in this study Zta1 was examined because it belongs to a
30 structurally distinct family of quinone reductases that are highly conserved in eukaryotes and
31 have been called the ζ -crystallins. The levels of Zta1 in *C. albicans* rapidly increased after
32 exposure to oxidants, consistent with a role in resisting oxidative stress. Accumulation of
33 reactive oxygen species was significantly higher in cells lacking *ZTA1* upon exposure to
34 quinones and other oxidants. Furthermore, deletion of *ZTA1* in a mutant lacking the four
35 flavodoxin-like proteins, resulted in further increased susceptibility to quinones, indicating that
36 these distinct quinone reductases work in combination. These results demonstrate that Zta1
37 contributes to *C. albicans* survival after exposure to oxidative conditions, which increases the
38 understanding of how *C. albicans* resists stressful conditions in the host.

39

40 **IMPORTANCE**

41 *Candida albicans* is an important human pathogen that can cause lethal systemic
42 infections. The ability of *C. albicans* to colonize and establish infections is closely tied to its
43 highly adaptable nature and capacity to resist various types of stress, including oxidative stress.
44 Previous studies showed that four *C. albicans* proteins belonging to the flavodoxin-like protein
45 family of quinone reductases are needed for resistance to quinones and for virulence.
46 Therefore, in this study we examined the role of a distinct type of quinone reductase, Zta1, and
47 found that it acts in conjunction with the flavodoxin-like proteins to protect against oxidative
48 stress.

49 **INTRODUCTION**

50 *Candida albicans* is a commensal organism that can grow on the skin and mucosa of
51 healthy individuals, but under certain circumstances it can overgrow and spread to cause
52 severe mucosal infections or lethal systemic infections (1). In order to be an effective pathogen,
53 *C. albicans* must resist stressful conditions to survive in the host, such as elevated temperature,
54 oxidative and nitrosative stress, antimicrobial peptides, and regulation of micronutrients, such as
55 iron depletion or copper toxicity (2-5). One important type of stress encountered *in vivo* is
56 caused by reactive oxygen species (ROS), which damage DNA, lipids and proteins and lead to
57 cell death (6). *C. albicans* uses an array of antioxidant mechanisms to deal with ROS, such as
58 superoxide dismutase, catalase, thioredoxin and glutathione (1).

59 Recently, a new antioxidant pathway was described in *C. albicans* involving four
60 flavodoxin-like proteins (FLPs; Pst1, Pst2, Pst3 and Ycp4) that are important for resisting
61 oxidative stress, preventing lipid peroxidation, and for virulence in mice (7, 8). The FLPs belong
62 to a large family of NADPH:quinone oxidoreductases that are present in many organisms,
63 including bacteria, fungi, and plants, but are not conserved in mammals (9). FLPs are enriched
64 in plasma membrane eisosome domains where they are thought to protect the *C. albicans*
65 plasma membrane by reducing ubiquinone to ubiquinol so that it can reduce reactive oxygen
66 species (7). FLPs are also important for resisting oxidative stress caused by treatment of *C.*
67 *albicans* with a variety of smaller quinone molecules (7, 8). FLPs are thought to therefore play a
68 critical role in protecting cells from quinones that are created as secondary metabolites, or in
69 many cases are used by plants and insects as defense molecules (10-12). Due to their redox-
70 active nature, quinones can cause oxidative stress by undergoing cycles of oxidation and
71 reduction, which can consume reducing agents such as glutathione and NADPH. In addition,
72 FLPs carry out a two-electron reduction of quinones, which prevents the formation of dangerous
73 semiquinone radicals that interact with oxygen to form superoxide anion radicals, leading to cell
74 damage (10, 11).

75 In addition to FLPs, many organisms contain members of a distinct group of quinone
76 oxidoreductases (QORs) that belong to the medium-chain dehydrogenase/reductase (MDR)
77 superfamily (13, 14). The first QOR of this group to be described was the mammalian ζ -
78 crystallin, a major protein of the eye lens that was observed to also be present in other cell
79 types where it is capable of reducing quinones using NADPH as a cofactor (15-18). However,
80 unlike the FLPs, it is believed that these enzymes catalyze a one-electron reduction of quinones
81 (16). A ζ -crystallin homologous protein called Zta1 has been described in *Saccharomyces*
82 *cerevisiae* and *Pichia pastoris*, and it has been suggested that it acts as a NADPH:quinone
83 oxidoreductase that protects cells from oxidative stress (17, 18). However, little is known about
84 it since data are limited for *S. cerevisiae* Zta1 and *C. albicans* Zta1 has not been studied
85 previously. Therefore, in this study we examined the production of Zta1 and its function in
86 protecting *C. albicans* from oxidative stress. In addition, a mutant lacking *ZTA1* as well as the
87 four flavodoxin-like proteins (*zta1* Δ *pst1* Δ *pst2* Δ *pst3* Δ *ycp4* Δ) was constructed to determine the
88 phenotype of a cell lacking all 5 QOR genes. These data indicate that Zta1 acts in combination
89 with FLPs to protect *C. albicans* from oxidative stress.

90

91 **RESULTS**

92 **Zta1 proteins are highly conserved between *C. albicans* and other fungi**

93 The medium-chain dehydrogenase/reductase family includes the QOR known as ζ -
94 crystallin that was first discovered in the lenses of camels and guinea pigs, but was
95 subsequently found in a wide range of eukaryotic cells (19). Interestingly, a protein with
96 homology to ζ -crystallin was identified in fungi. The crystal structure of the *Saccharomyces*
97 *cerevisiae* ζ -crystallin, termed Zta1, has been described and shows that it is structurally similar
98 to mammalian ζ -crystallin proteins (20). Comparison of the Zta1 proteins from *S. cerevisiae* and
99 *C. albicans* revealed a high degree of sequence identity (56.8%) and there was 100%
100 conservation of residues implicated in catalytic activity (Fig. 1). Although the human homolog
101 Cryz has low overall sequence identity to Zta1 (~26%), the active site residues are mostly
102 conserved. Therefore, *C. albicans* Zta1 belongs to the highly conserved family of ζ -crystallin
103 proteins.

104

105 **Zta1 is localized to the cytoplasm and induced by oxidation**

106 To examine the subcellular localization and production of Zta1, a triple GFP tag (3xGFP)
107 was fused to the 3' end of the *ZTA1* open reading frame. Analysis of log-phase cells by
108 fluorescence microscopy revealed that Zta1-3xGFP localized to the cytoplasm. The basal level
109 of Zta1-3xGFP was low in cells grown in standard medium, but the signal was induced by the
110 treatment with several different quinones including p-benzoquinone (BZQ) (4-fold), 2-tert-butyl-
111 1,4-benzoquinone (TBBQ) (1.6-fold), and menadione (MEN) (2.5-fold). (Fig. 2A, D).
112 Interestingly, H_2O_2 also significantly increased Zta1 production (3.5-fold), indicating that *ZTA1*
113 expression is induced by oxidative stress, not just by quinones. Concentrations as low as 10 μM
114 BZQ were sufficient to achieve a 3-fold increase in Zta1-3xGFP production (Fig. 2B, E).
115 Treatment with 100 μM BZQ resulted in a reduction of Zta1-3xGFP induction, probably due to

116 toxicity. *ZTA1* was induced quickly after exposure to BZQ. The relative level of Zta1-3xGFP
117 increased by 2-fold and 3.1-fold increase after 30 and 60 minutes, respectively (Fig 2C, F).

118 Since Zta1-3xGFP was localized to the cytoplasm, Western blot analysis was carried out
119 to determine whether the expected fusion protein was produced or if free GFP was being
120 proteolytically clipped off. A band of ~118 kDa was detected with anti-GFP antibodies,
121 indicating the full length Zta1-3xGFP fusion protein was produced. Only a weak signal was
122 detected at the expected position for free GFP (~26.7kDa), confirming that Zta1-3xGFP is
123 cytoplasmic.

124 Western blot analysis also detected increased production of Zta1-3xGFP after 1 hour
125 induction with BZQ (2.3-fold), MEN (2.8-fold) and H₂O₂ (2.6-fold) (Fig. 3A). However, treatment
126 with 100 μ M TBBQ led to lower Zta1 induction (0.6-fold), probably due to greater toxicity. This
127 was corroborated by results showing that TBBQ induced significantly more cell death after 1 h
128 incubation than the other compounds (Fig. 3D). Additional analyses confirmed that Zta1 is
129 induced by low concentrations of BZQ (2.5-fold at 10 μ M; 3.9-fold at 30 μ M) but starts to
130 decrease at 100 μ M (1.8-fold) (Fig. 3B). A rapid increase in Zta1 levels was observed after 15
131 minutes (3.6-fold), increasing to 6-fold after 30 minutes and by more than 10-fold after 1 hour of
132 BZQ treatment (Fig. 3C). These data demonstrate Zta1 is rapidly induced by oxidizing agents.

133

134 **Zta1 prevents accumulation of reactive oxygen species**

135 The ability of Zta1 to protect against ROS was examined using the fluorescent probe
136 H₂DCFDA, which has been previously used to quantify ROS accumulation in *Candida* cells (21).
137 Wild type and *zta1* Δ/Δ mutant cells treated with 30 μ M of the quinones BZQ and TBBQ did not
138 lead to detectable accumulation of ROS using H₂DCFDA (Fig. 4A, D). However, both quinones
139 significantly induced ROS accumulation at 100 μ M in the *zta1* Δ/Δ mutant, which was abolished
140 in the complemented strain *zta1*⁺ (Fig. 4B, C, E, F). The median fluorescence intensity of *zta1* Δ/Δ
141 cells that were incubated with TBBQ was significantly higher when compared with cells exposed

142 to BZQ (*t* test $P= 0.021$). These data indicate Zta1 can reduce ROS accumulation caused by
143 quinones and protect *C. albicans* from oxidative damage, and that TBBQ induces higher
144 production ROS than does BZQ in the *zta1Δ/Δ* cells.

145

146 **Zta1 acts in combination with the FLPs to protect *C. albicans* from quinones**

147 To determine whether Zta1 is important for *C. albicans* resistance to quinones, we
148 compared a wild-type *C. albicans* control strain with the *zta1Δ/Δ* mutant and the complemented
149 strain *zta1+*. However, no differences in sensitivity were detected with disk diffusion halo
150 assays when the strains were exposed to BZQ, MEN or TBBQ. Since *C. albicans* also possess
151 QORs that belong to the FLP family, we tested whether *ZTA1* might be more important in the
152 absence of the FLPs. *ZTA1* was deleted from a quadruple mutant lacking all four FLPs (*pst1Δ/Δ*
153 *pst2Δ/Δ* *pst3Δ/Δ* *ycp4Δ/Δ*; referred to as $\Delta/\Delta/\Delta/\Delta$ for simplicity) (7) to create a quintuple mutant
154 lacking the four FLPs and *ZTA1* (referred to as Q Mut). We also generated a Q mutant
155 complemented with *ZTA1* (*pst1Δ/Δ* *pst2Δ/Δ* *pst3Δ/Δ* *ycp4Δ/Δ* *zta1Δ/Δ* + *ZTA1*; referred to as Q
156 Mut+). Although no difference was observed when cells were treated with BZQ or MEN, the Q
157 Mut was more sensitive to killing by TBBQ when compared with the $\Delta/\Delta/\Delta/\Delta$ mutant, and this
158 sensitivity was partially reverted in the Q Mut+ complemented with *ZTA1* (Fig. 5). Perhaps
159 TBBQ is more effective at killing *C. albicans* because it is more nonpolar than the other
160 quinones used in this study and may therefore cross membranes more efficiently. These data
161 indicate that Zta1 synergizes with the FLPs to detoxify certain quinones.

162

163 **Zta1 protection appears to be specific to quinones**

164 To determine if Zta1 protects *C. albicans* against other sources of oxidative stress, the
165 susceptibility of cells to other oxidizing agents was examined including H_2O_2 , tert-Butyl-
166 hydroperoxide (Fig. 6) and the thiol oxidizing compound diamide (data not shown). Neither
167 *zta1Δ/Δ* nor the Q Mut strain showed increased susceptibility to these other oxidizing agents

168 (Figure 6). Thus, although Zta1 is induced by H₂O₂, it does not appear to play a major role in
169 protecting against this type of oxidative stress.

170

171 ***zta1Δ/Δ shows a trend of increased susceptibility to killing by neutrophils***

172 To assess the potential significance of *ZTA1* in *C. albicans* resistance to attack by the
173 immune system, we analyzed the ability of human neutrophils to kill *C. albicans* wild-type and
174 mutant strains. Notably, increased vulnerability of *zta1Δ/Δ* cells to neutrophil-mediated killing
175 was observed, which was reversed in the *ZTA1* complemented strain (Fig. 7). Unfortunately,
176 due to variation in the data, this trend did not reach statistical significance when analyzed by
177 ANOVA or t-test. Donor-dependent variations when working with neutrophils are known to
178 occur, since environmental aspects such as temperature, pH, oxygen and glucose levels can
179 have a strong influence in the function of neutrophils (22). Deletion of the *ZTA1* gene in the
180 Δ/Δ/Δ/Δ mutant did not yield an obvious increase in susceptibility to neutrophils; similar survival
181 levels were observed between the *zta1Δ/Δ*, Δ/Δ/Δ/Δ, Q mut and Q mut+ (complemented with
182 *ZTA1*).

183

184 ***ZTA1 role in C. albicans virulence***

185 The role of *ZTA1* in *C. albicans* virulence was investigated in a mouse model of
186 hematogenously disseminated candidiasis (23). The wild-type, Δ/Δ/Δ/Δ, Q Mut and Q Mut+
187 strains were used infect BALB/c mice via tail vein injection with 2.5 x 10⁵ *C. albicans* cells. Since
188 it has been shown that the Δ/Δ/Δ/Δ mutant is non-virulent and is cleared after ~4 days of
189 infection (7), we focused on measuring the colony forming units in the kidney (CFU/g kidney)
190 after 2 and 3 days of infection. The kidneys are an established target organ for testing the
191 capacity of *C. albicans* to cause an infection, since growth occurs rapidly in the kidneys during
192 the first 2 days after injection (24). Interestingly, at day 2 (Fig. 8A) and 3 (Fig. 8B) post infection,
193 the Q Mut strain showed lower CFU/g kidney than did the Δ/Δ/Δ/Δ strain, suggesting a role for

194 *ZTA1* in virulence. In contrast, the Q Mut+ strain had similar fungal burden as the $\Delta/\Delta/\Delta/\Delta$,
195 indicating this effect was reversed by reintroducing the *ZTA1* gene. However, this trend in the
196 results did not reach statistical significance when analyzed by ANOVA or t-test. Nonetheless,
197 the $\Delta/\Delta/\Delta/\Delta$ and Q Mut strains had lower kidney fungal burden than the wild-type control strain,
198 highlighting the importance of quinone reductases in virulence. Although statistical significance
199 was lacking, the overall trends of these studies suggest that *Zta1* contributes to *C. albicans*
200 virulence.

201

202 **DISCUSSION**

203 Fungal cells face various challenges when colonizing a host, including reactive oxygen
204 species (ROS) that can cause widespread damage to proteins, lipids, and nucleic acids (25).
205 Among the arsenal employed by fungal cells to deal with this stress are quinone oxidoreductase
206 (QOR) enzymes capable of reducing quinones into hydroquinones (13). This mechanism holds
207 significance as quinones have the potential to alkylate proteins and DNA or undergo
208 autoxidation, resulting in the production of semiquinone radicals and the generation of ROS (9,
209 11, 26, 27). Furthermore, QORs can also reduce ubiquinone, a well-known component of the
210 mitochondrial membrane that participates in cellular respiration, but is also present in other
211 membranes, including the plasma membrane, where it functions as an antioxidant (28). In fact,
212 recent studies revealed that four members of the FLP family of flavin-dependent
213 NADPH:quinone oxidoreductases (Pst1, Pst2, Pst3, Ycp4) are needed for resistance to
214 quinones and virulence (7). The FLP family members in *C. albicans* are thought to act in part by
215 catalyzing a two-electron reduction of ubiquinone that enable it to then reduce ROS in the
216 plasma membrane (7). The FLPs are localized to specialized plasma membrane domains called
217 eisosomes, which is thought to facilitate a role in protecting the *C. albicans* plasma membrane
218 polyunsaturated fatty acids (PUFAs) which are more prone to lipid peroxidation. This type of
219 lipid oxidation can trigger a chain reaction that spreads to other PUFAs and then the peroxidized
220 lipids can damage proteins and DNA (8, 29). Another QOR present in fungi is the ζ -crystallin-
221 like protein Zta1, which belongs to a structurally distinct family that is believed to catalyze a one-
222 electron reduction of quinones (16, 18). Due to the FLPs importance, we decided to investigate
223 the role of Zta1 in *C. albicans*.

224 The high degree of amino acid conservation in the active site of *C. albicans* Zta1 strongly
225 indicates that it functions as a QOR, as in *S. cerevisiae* (Fig. 1). Supporting this notion, *C. albicans*
226 Zta1 was rapidly induced upon exposure to p-benzoquinone (BZQ), 2-tert-butyl-1,4-
227 benzoquinone (TBBQ), menadione (MEN) and hydrogen peroxide (H_2O_2) (Figs. 2 and 3).

228 However, despite its induction by H₂O₂, Zta1 does not appear to play a significant role in protecting
229 cells against H₂O₂ or other oxidants such as tert-butyl-hydroperoxide (Fig. 6) and diamide (data
230 not shown). Previous studies have reported the upregulation of flavin-containing QORs under
231 certain conditions, such as increased temperature (26). Moreover, Zta1 production in *S.*
232 *cerevisiae* increased following treatment with rapamycin, heat shock and during the stationary
233 phase, when cells are starved, and toxic compounds accumulate (30). These observations
234 suggest that Zta1 may be part of a more general fungal cellular response to stress, which could
235 explain its induction by H₂O₂ while not directly providing protection against it.

236 Assays utilizing H₂DCFDA revealed that the *zta1Δ/Δ* exhibited increased accumulation of
237 ROS upon exposure to quinones, indicating it protects against this type of oxidative stress (Fig.
238 4). Surprisingly, we did not observe increased cell death of the *zta1Δ/Δ* mutant in response to
239 quinones, despite a previous report that the *S. cerevisiae* *zta1Δ* mutant showed slightly increased
240 susceptibility to menadione (18). However, the Q Mut, which lacks all four FLPs
241 (*pst1Δ/pst2Δ/pst3Δ/ycp4Δ*) as well as *ZTA1*, exhibited greater susceptibility to TBBQ, although
242 not to BZQ or MEN. One possibility for this specific susceptibility is that TBBQ, being the most
243 non-polar quinone tested in our study (8), may cross the plasma membrane more readily and
244 enter the cytoplasm where Zta1 is located (Fig. 2). In this scenario, *C. albicans* FLPs may
245 preferentially act at the plasma membrane where they are localized and Zta1 may be important
246 to reduce TBBQ in the cytoplasm, where it was detected.

247 To determine if *ZTA1* is important for *C. albicans* to avoid attack by the immune system,
248 the *zta1ΔΔ* mutant was assessed for its ability to survive incubation with human neutrophils. The
249 results showed a trend of increased killing of the *zta1ΔΔ* mutant by neutrophils, which was
250 reversed by reintroduction of the *ZTA1* gene in the complemented strain (Fig. 7). The presence
251 or absence of *ZTA1* in cells lacking all four FLPs did not appear to obviously impact in *C. albicans*
252 survival, perhaps because cells lacking the FLPs are already more susceptible to neutrophils.

253 Previous studies demonstrated that the FLPs are critical for *C. albicans* infection in mice,
254 as a mutant lacking all four FLPs was avirulent and cleared from the kidney at early times after
255 infection that correlated with the influx of neutrophils (7). Considering the limited role of *zta1Δ/Δ*
256 in susceptibility to quinones in vitro, we decided to investigate whether *zta1Δ/Δ* would exacerbate
257 the previously described virulence defect of the FLP mutant (*pst1Δ/Δ* *pst2Δ/Δ* *pst3Δ/Δ* *ycp4Δ/Δ*)
258 (7) by assessing the kidney fungal burden in infected mice. Notably, we observed a trend towards
259 reduced CFU/g kidney of the Q Mut at both day 2 and day 3 post-infection. Complementation of
260 Q Mut with *ZTA1* restored its clearance to levels comparable to those of the FLP mutant. This
261 finding aligns with studies implicating QORs in the virulence of other organisms, such as
262 *Xanthomonas citri*, *Mycobacterium tuberculosis* and *Staphylococcus aureus* (31-33). This
263 suggests that Zta1 contributes, at least partially, to *C. albicans* ability to resist in the host and
264 evade its immune system.

265 Collectively, our data indicate that Zta1 is rapidly induced by quinones and protects *C.*
266 *albicans* against quinone-induced damage. It also protects against the accumulation of ROS
267 caused by quinones and might contribute to *C. albicans* capacity to establish an infection. Zta1
268 function seems to overlap with other QORs, such as the FLPs, and due to their difference in
269 localization, they seem to complement each other. These results highlight the important role of
270 QORs in *C. albicans* repertoire of strategies to be a successful pathogen.

271

272 **METHODS**

273 **Strains and media**

274 *C. albicans* strains used are listed in Table 1. Strains were kept in YPD (1% yeast
275 extract, 2% peptone, 2% glucose) agar plates. Prior to experiments, cultures were grown in
276 YPD medium (2% dextrose, 1% peptone, 2% yeast extract, 80 mg/L uridine) (34). A 3xGFPy tag
277 was fused to the 3' end of the open reading frame of *ZTA1* by homologous recombination as
278 previously described (35, 36). The DNA was introduced into *C. albicans* cells by electroporation
279 and allowed to recombine with the homologous regions of the *ZTA1* gene. Strains were verified
280 by PCR analysis and microscopic examination of GFPy fluorescence in a Zeiss Axiovert 200M
281 microscope equipped with an AxioCam HRm camera and Zeiss ZEN software. Mutant strains of
282 *zta1* were generated using a transient expression of CRISPR-Cas9 to obtain homozygous
283 deletion of the target gene, as previously described (37). A 20-bp target sequence of the sgRNA
284 was used to delete *ZTA1* in strain SN152, and primers were designed to include 80 bases of
285 homology to the sequences of target gene. The gene was deleted with by replacement with a
286 *HIS1* selectable marker. For the Q Mut, *ZTA1* was deleted and replaced with an *ARG4*
287 selectable marker in strain LLF054. The complemented strains of *ZTA1* were obtained by
288 integrating a copy of the wild-type gene sequence into the *NEUT5L* region of the genome using
289 the gap-repair method, as previously described (38). The PCR fragment was constructed by
290 amplification of the genomic DNA from 0.5kb upstream of the start codon and 0.25kb
291 downstream of the stop codon of the *ZTA1* gene from *C. albicans* SC5314 using primers 5227
292 and 5228, which includes 20-bp homology to the *ZTA1* upstream and downstream regions and
293 40-bp homology with the plasmid pDIS3, that carries the *NAT1* resistance cassette. The PCR
294 fragment was recombined into *Sma*I-digested pDIS3 in *S. cerevisiae* strain L40, generating the
295 pDIS3-*ZTA1*-*NAT1* construct, which was subsequently released from the pDIS3 vector by *Sfi*
296 digestion and transformed into the *zta1Δ/Δ* or Q Mut strain by electroporation. The primers used
297 are listed on Table 2.

298 **Sequence alignments of Zta1 proteins**

299 Zta1 protein sequence was obtained from the *S. cerevisiae* Genome Database
300 (<http://www.yeastgenome.org>). BLAST searches were carried out to identify Zta1 homologues in
301 the *C. albicans* Genome Database (<http://www.candidagenome.org>) and genome sequences
302 present at the Web site of the National Center for Biotechnology
303 (<http://www.ncbi.nlm.nih.gov/BLAST/>). Multiple sequence alignments of the predicted Zta1
304 proteins were carried out using Jalview (39).

305

306 **Microscopic analysis of Zta1-3xGFP γ production**

307 3xGFP γ tagged *C. albicans* strains were grown overnight in YPD at 30°C and then
308 diluted 1:250 in 5 mL YPD and grown until a density of about 1 X 10⁷ cells/ml. Cells (1 mL) were
309 treated with 100 μ M of one of the quinones p-benzoquinone (BZQ; Sigma-Aldrich, St. Louis,
310 MO), 2-tert-butyl-1,4-benzoquinone (TBBQ; Cayman Chemical, Ann Arbor, MI), menadione
311 (MND; Sigma-Aldrich, St. Louis, MO) or 500 μ M of H₂O₂ and incubated for 1h at 30°C on a tube
312 roller. Samples were centrifuged, washed in sterile phosphate-buffered saline (PBS), and
313 analyzed by fluorescence microscopy. To assess the effect on Zta1 production of different times
314 and concentrations of incubation with BZQ, cells were treated with 10, 30 or 100 μ M of BZQ, or
315 treated with 100 μ M of BZQ for 15, 30 and 60 minutes of incubation and then prepared for
316 imaging as described above. Zeiss ZEN software was used to control the microscope and for
317 deconvoluting images and calculating the mean fluorescence intensity (MFI) of cells. Statistical
318 analysis of MFI compared to non-treated GFP-tagged cells was carried out with Prism 6
319 software (GraphPad Software, Inc., La Jolla, CA).

320

321 **Western blot analysis of Zta1-3xGFP γ levels**

322 The same protocol described above was used for western blot analysis. Shortly, 1 X 10⁷
323 cells/ml were treated with 100 μ M of BZQ, TBBQ, MEN or 500 μ M of H₂O₂ and incubated for 1h

324 at 30°C shaking before being harvested. The same process was used for cells treated with 10,
325 30 or 100 μ M of BZQ for 1h or cells treated with 100 μ M of BZQ for 15, 30 or 60 minutes. Cell
326 lysates were prepared by bead-bashing as follows: 20 mL of cell culture prepared as described
327 above were centrifuged, washed with PBS and lysed using 300 μ l of 1x Laemmli buffer (2%
328 SDS, 10% glycerol, 125 mM Tris-HCl, pH 6.8, and 0.002% bromophenol blue, 5% 2-
329 Mercaptoethanol) and zirconia beads by 5 rounds of 1 min of bead beating followed by 1 min on
330 ice. Samples (10 μ l) were separated by SDS-PAGE and transferred to a 0.4 mm nitrocellulose
331 membrane using a semidry transfer apparatus. Blots were probed for 1h at room temperature
332 (RT) with a mouse anti-GFP antibody (Living Colors -JL-8, BD Biosciences Clontech) in TBS-T
333 buffer (20 mM Tris, 150 mM NaCl, 0.1% Tween 20, 2% [wt/vol] bovine serum albumin [BSA],
334 and 0.2% [wt/vol] sodium azide). The blots were then washed and incubated for 1h with an
335 IRDye 800-conjugated anti-mouse IgG (LI-COR Biosciences, Lincoln, NE) diluted 1:15,000 in
336 TBS (20 mM Tris, 150 mM NaCl) containing 0.5% Tween 20. Blots were washed using TBS-T
337 and visualized by scanning with an Odyssey CLx infrared imaging system (LI-COR
338 Biosciences). The resulting images were analyzed using Image Studio software (LI-COR
339 Biosciences). For Coomassie-stained gels, SDS-PAGE was performed as described above, and
340 then gels were stained in a Coomassie brilliant blue solution (0.1% Coomassie R-250, 40%
341 ethanol, 10% glacial acetic acid) overnight. Gels were destained in destaining solution (40%
342 methanol, 10% acetic acid) and analyzed using Image Studio software (LI-COR Biosciences).
343 Statistical analysis of densitometry was carried out with Prism 6 software (GraphPad Software,
344 Inc., La Jolla, CA) using multiple *t* tests against non-treated GFP-tagged cells.
345

346 **Sensitivity to oxidizing agents**

347 *C. albicans* strains were grown overnight in YPD at 30°C were diluted to 2.5×10^5 cells
348 were spread onto the surface of a synthetic complete medium agar plate. 10 μ l of each
349 compound was applied to paper filter disks (Becton, Dickinson and Company, Sparks, MD), the

350 disks were applied to the plates surface, incubated at 30°C for 48 h, and then the diameter of
351 the zone of growth inhibition (halo) was measured. Compounds tested included p-benzoquinone
352 (BZQ; Sigma-Aldrich, St. Louis, MO), menadione (MND; Sigma-Aldrich, St. Louis, MO), 2-tert-
353 butyl-1,4-benzoquinone (TBBQ; Cayman Chemical, Ann Arbor, MI), hydrogen peroxide (H₂O₂;
354 Sigma-Aldrich, St. Louis, MO), tert-Butyl hydroperoxide (tBOOH – Acros Organics) and diamide
355 (Sigma-Aldrich, St. Louis, MO). For the CFU assays, wild-type and the 3xGFP-tagged strains
356 were grown overnight, harvested by centrifugations, and resuspended in PBS. A total of 1 X 10⁷
357 cells/ml were inoculated in liquid YPD and treated with one of the following: 100 µM of p-
358 benzoquinone, 100 µM 2-tert-butyl-1,4-benzoquinone, 100 µM menadione or 500 µM of
359 hydrogen peroxide. Tubes were incubated for 1 h at 30°C on a tube roller, after which cultures
360 were centrifugated and cells washed twice with PBS. Serial dilutions were plated in YPD plates
361 and incubated for 48h at 30°C, and colony forming units were counted.

362

363 **ROS accumulation**

364 *C. albicans* (WT, *zta1Δ/Δ* and *zta1+*) was grown overnight in 5 mL of YPD. The following
365 day. cultures were diluted to 0.100 OD into 5 ml of fresh YPD and grown for 2h at 30°C
366 agitating. BZQ or TBBQ (10, 30 and 100 µM/mL) were added, and cultures incubated for an
367 additional 1 h. After that, H₂DCFDA (10 µM/mL) was added, and cultures were incubated for 20
368 minutes in the dark at 30°C with shaking. Cultures were centrifuged, washed twice with PBS
369 and resuspended in 100µL of PBS. Samples were analyzed by microscopy at 492nm in a Zeiss
370 Axiovert 200M microscope equipped with an AxioCam HRm camera and Zeiss ZEN software for
371 deconvolving images.

372

373 **Human neutrophil killing of *C. albicans*.**

374 Blood was obtained from study participants with written informed consent through a
375 protocol approved by the University of Wisconsin Internal Review Board. Neutrophils were

376 isolated from 4 different donors using the MACSxpress Neutrophil Isolation and MACSxpress
377 Erythrocyte Depletion kits (Miltenyi Biotec Inc., Auburn, CA) and suspended in RPMI 1640
378 (without phenol red) supplemented with 2% heat-inactivated fetal bovine serum (FBS) and
379 supplemented with glutamine (0.3 mg/ml) as previously described (40). For the killing assays,
380 neutrophils (4×10^5 cells) and the *C. albicans* strains (1×10^6 cells) were added to wells of a
381 culture treated 96-well flat-bottom plate and incubated for 4 h at 37°C in 5% CO₂. After
382 incubation, 10 µg of DNase1 was added to each well and the plate was incubated at 37°C with
383 5% CO₂ for 10 minutes, after which contents of the wells (media and non-adherent cells) were
384 moved into a 96-well round-bottom plate. Some neutrophils and *C. albicans* cells can adhere to
385 the flat-bottom plate, so the contents of both the flat-bottom plate and the round-bottom plate
386 were processed and combined back in the flat-bottom plate for the analysis. The round-bottom
387 plate was centrifuged at 1,200xg for 2 min, the supernatant was discarded and 150 µl of ddH₂O
388 containing 1 µg/ml DNase1 was added to each well of the round-bottom and the flat-bottom
389 plate. Plates were incubated at 37°C for 20 minutes to lyse neutrophils. The round-bottom plate
390 was centrifuged at 1,200xg and the supernatant removed, after which the contents of the
391 original flat-bottom plate were removed and used to resuspend the contents of their respective
392 wells in the round-bottom plate. The lysis step was repeated one additional time, after which the
393 round-bottom plate was centrifuged at 1,200xg, the supernatant removed, and the remaining
394 yeast cells were resuspended in 100 µl of RPMI + 2% FBS and transferred to the original wells
395 of the 96-well flat-bottom plate. Then, 10 µl PrestoBlue (Invitrogen, Eugene, OR) was added to
396 each well, gently mixed, and plate was incubated for 25 min at 37°C. Fluorescence 560/590
397 was then read on a BioTek Synergy|H1 microplate reader (Agilent, Santa Clara, CA).
398 Percentage of viable *C. albicans* cells was quantified by calculating the fluorescence signal of
399 the treated well (mutant and neutrophils) as a percentage of the control well (same mutant and
400 no neutrophils).
401

402 **Mouse infection assays**

403 Fungal burden was tested in mice as previously described (24) using a protocol
404 approved by the Stony Brook University IACUC committee. Strains were grown overnight in
405 YPD medium, reinoculated into fresh medium and incubated again overnight. Cells were
406 harvested after centrifugation and washed twice with PBS and counted using a hemocytometer.
407 Cells were diluted to 1.25×10^6 cells/ml with PBS. Female BALB/c mice (8 weeks old) were
408 injected via the lateral tail vein with 2.5×10^5 cells (200 μ l). After 48h or 72h, kidneys were
409 excised, weighed, and then homogenized in 5 ml PBS for 30 s with a tissue homogenizer (Pro
410 Scientific Inc.). The CFU per gram of kidney (CFU/g kidney) was determined by plating dilutions
411 of the homogenates on YPD agar medium plates and incubating for 2 days at 30°C. Statistical
412 analysis of the CFU data was carried out with Prism 6 software (GraphPad Software, Inc., La
413 Jolla, CA) using one-way analysis of variance with one-way ANOVA.

414

415 **ACKNOWLEDGMENTS**

416 We thank the members of our lab for their helpful advice and suggestions on this study.
417 This research was supported by Public Health Service grants awarded from the National
418 Institute of Health to J.B.K (R01AI047837) and to J.E.N (R01AI145939 and R21AI159583).

419

420 **CONFLICTS OF INTEREST**

421 The authors declare that they do not have any conflicts of interest relating to this
422 research project.

423 **REFERENCES**

- 424 1. Dantas Ada S, Day A, Ikeh M, Kos I, Achan B, Quinn J. 2015. Oxidative stress
425 responses in the human fungal pathogen, *Candida albicans*. *Biomolecules* 5:142-65.
- 426 2. Brown AJ, Budge S, Kaloriti D, Tillmann A, Jacobsen MD, Yin Z, Ene IV, Bohovych I,
427 Sandai D, Kastora S, Potrykus J, Ballou ER, Childers DS, Shahana S, Leach MD. 2014.
428 Stress adaptation in a pathogenic fungus. *J Exp Biol* 217:144-55.
- 429 3. Douglas LM, Konopka JB. 2019. Plasma membrane architecture protects *Candida*
430 *albicans* from killing by copper. *PLoS Genet* 15:e1007911.
- 431 4. Tripathi A, Liverani E, Tsygankov AY, Puri S. 2020. Iron alters the cell wall composition
432 and intracellular lactate to affect *Candida albicans* susceptibility to antifungals and host
433 immune response. *J Biol Chem* 295:10032-10044.
- 434 5. Lanze CE, Zhou S, Konopka JB. 2021. The Sur7 cytoplasmic C terminus regulates
435 morphogenesis and stress responses in *Candida albicans*. *Mol Microbiol* 116:1201-
436 1215.
- 437 6. Brown AJ, Haynes K, Quinn J. 2009. Nitrosative and oxidative stress responses in
438 fungal pathogenicity. *Curr Opin Microbiol* 12:384-91.
- 439 7. Li L, Naseem S, Sharma S, Konopka JB. 2015. Flavodoxin-Like Proteins Protect
440 *Candida albicans* from Oxidative Stress and Promote Virulence. *PLoS Pathog*
441 11:e1005147.
- 442 8. Foderaro JE, Konopka JB. 2021. Differential Roles of a Family of Flavodoxin-Like
443 Proteins That Promote Resistance to Quinone-Mediated Oxidative Stress in *Candida*
444 *albicans*. *Infect Immun* 89.
- 445 9. Moyo CE, Minibayeva F, Liers C, Beckett RP. 2021. Role of quinone reductases in
446 extracellular redox cycling in lichenized ascomycetes. *Fungal Biol* 125:879-885.
- 447 10. Franzia T, Gaudu P. 2022. Quinones: more than electron shuttles. *Res Microbiol*
448 173:103953.
- 449 11. Bolton JL, Dunlap T. 2017. Formation and Biological Targets of Quinones: Cytotoxic
450 versus Cytoprotective Effects. *Chem Res Toxicol* 30:13-37.
- 451 12. Christiansen JV, Isbrandt T, Petersen C, Sondergaard TE, Nielsen MR, Pedersen TB,
452 Sorensen JL, Larsen TO, Frisvad JC. 2021. Fungal quinones: diversity, producers, and
453 applications of quinones from *Aspergillus*, *Penicillium*, *Talaromyces*, *Fusarium*, and
454 *Arthrinium*. *Appl Microbiol Biotechnol* 105:8157-8193.
- 455 13. Yang C, Huang Z, Zhang X, Zhu C. 2022. Structural Insights into the NAD(P)H:Quinone
456 Oxidoreductase from *Phytophthora capsici*. *ACS Omega* 7:25705-25714.
- 457 14. Oppermann U. 2007. Carbonyl reductases: the complex relationships of mammalian
458 carbonyl- and quinone-reducing enzymes and their role in physiology. *Annu Rev
459 Pharmacol Toxicol* 47:293-322.
- 460 15. Borras T, Jornvall H, Rodokanaki A, Gonzalez P, Rodriguez I, Hernandez-Calzadilla C.
461 1990. The transcripts of zeta-crystallin, a lens protein related to the alcohol
462 dehydrogenase family, are altered in a guinea-pig hereditary cataract. *Exp Eye Res*
463 50:729-35.

464 16. Rao PV, Krishna CM, Zigler JS. 1992. Identification and characterization of the
465 enzymatic activity of zeta-crystallin from guinea pig lens. A novel NADPH:quinone
466 oxidoreductase. *Journal of Biological Chemistry* 267:96-102.

467 17. Fernandez MR, Porte S, Crosas E, Barbera N, Farres J, Biosca JA, Pares X. 2007.
468 Human and yeast zeta-crystallins bind AU-rich elements in RNA. *Cell Mol Life Sci*
469 64:1419-27.

470 18. Porte S, Crosas E, Yakovtseva E, Biosca JA, Farres J, Fernandez MR, Pares X. 2009.
471 MDR quinone oxidoreductases: the human and yeast zeta-crystallins. *Chem Biol Interact*
472 178:288-94.

473 19. Huang QL, Russell P, Stone SH, Zigler JS, Jr. 1987. Zeta-crystallin, a novel lens protein
474 from the guinea pig. *Curr Eye Res* 6:725-32.

475 20. Guo PC, Ma XX, Bao ZZ, Ma JD, Chen Y, Zhou CZ. 2011. Structural insights into the
476 cofactor-assisted substrate recognition of yeast quinone oxidoreductase Zta1. *J Struct*
477 Biol 176:112-8.

478 21. Gandra RM, Silva LN, Souto XM, Sangenito LS, Cruz LPS, Braga-Silva LA, Goncalves
479 DS, Seabra SH, Branquinha MH, Santos ALS. 2019. The serine peptidase inhibitor
480 TPCK induces several morphophysiological changes in the opportunistic fungal
481 pathogen *Candida parapsilosis* sensu stricto. *Med Mycol* 57:1024-1037.

482 22. Blanter M, Gouwy M, Struyf S. 2021. Studying Neutrophil Function in vitro: Cell Models
483 and Environmental Factors. *J Inflamm Res* 14:141-162.

484 23. Spellberg B, Ibrahim AS, Edwards JE, Jr., Filler SG. 2005. Mice with disseminated
485 candidiasis die of progressive sepsis. *J Infect Dis* 192:336-43.

486 24. Naseem S, Frank D, Konopka JB, Carpino N. 2015. Protection from systemic *Candida*
487 *albicans* infection by inactivation of the Sts phosphatases. *Infect Immun* 83:637-45.

488 25. Alves R, Barata-Antunes C, Casal M, Brown AJP, Van Dijck P, Paiva S. 2020. Adapting
489 to survive: How *Candida* overcomes host-imposed constraints during human
490 colonization. *PLoS Pathog* 16:e1008478.

491 26. Cohen R, Suzuki MR, Hammel KE. 2004. Differential stress-induced regulation of two
492 quinone reductases in the brown rot basidiomycete *Gloeophyllum trabeum*. *Appl Environ*
493 *Microbiol* 70:324-31.

494 27. Gutierrez-Fernandez J, Kaszuba K, Minhas GS, Baradaran R, Tambalo M, Gallagher
495 DT, Sazanov LA. 2020. Key role of quinone in the mechanism of respiratory complex I.
496 *Nat Commun* 11:4135.

497 28. Wang Y, Hekimi S. 2016. Understanding Ubiquinone. *Trends Cell Biol* 26:367-378.

498 29. Yin H, Xu L, Porter NA. 2011. Free radical lipid peroxidation: mechanisms and analysis.
499 *Chem Rev* 111:5944-72.

500 30. Crosas E, Sumoy L, Gonzalez E, Diaz M, Bartolome S, Farres J, Pares X, Biosca JA,
501 Fernandez MR. 2015. The yeast zeta-crystallin/NADPH:quinone oxidoreductase (Zta1p)
502 is under nutritional control by the target of rapamycin pathway and is involved in the
503 regulation of argininosuccinate lyase mRNA half-life. *FEBS J* 282:1953-64.

504 31. Barcarolo MV, Garavaglia BS, Gottig N, Ceccarelli EA, Catalano-Dupuy DL, Ottado J.
505 2020. A novel *Xanthomonas citri* subsp. *citri* NADPH quinone reductase involved in salt
506 stress response and virulence. *Biochim Biophys Acta Gen Subj* 1864:129514.

507 32. Akhtar P, Srivastava S, Srivastava A, Srivastava M, Srivastava BS, Srivastava R. 2006.
508 Rv3303c of *Mycobacterium tuberculosis* protects tubercle bacilli against oxidative stress
509 in vivo and contributes to virulence in mice. *Microbes Infect* 8:2855-62.

510 33. Fuller JR, Vitko NP, Perkowski EF, Scott E, Khatri D, Spontak JS, Thurlow LR,
511 Richardson AR. 2011. Identification of a lactate-quinone oxidoreductase in
512 *Staphylococcus aureus* that is essential for virulence. *Front Cell Infect Microbiol* 1:19.

513 34. Sherman F. 1991. Getting started with yeast. *Methods Enzymol* 194:3-21.

514 35. Zhang C, Konopka JB. 2010. A photostable green fluorescent protein variant for analysis
515 of protein localization in *Candida albicans*. *Eukaryot Cell* 9:224-6.

516 36. Duenas-Santero E, Santos-Almeida A, Rojo-Dominguez P, Del Rey F, Correa-Bordes J,
517 Vazquez de Aldana CR. 2019. A new toolkit for gene tagging in *Candida albicans*
518 containing recyclable markers. *PLoS One* 14:e0219715.

519 37. Min K, Ichikawa Y, Woolford CA, Mitchell AP. 2016. *Candida albicans* Gene Deletion
520 with a Transient CRISPR-Cas9 System. *mSphere* 1.

521 38. Gerami-Nejad M, Zacchi LF, McClellan M, Matter K, Berman J. 2013. Shuttle vectors for
522 facile gap repair cloning and integration into a neutral locus in *Candida albicans*.
523 *Microbiology (Reading)* 159:565-579.

524 39. Waterhouse AM, Procter JB, Martin DM, Clamp M, Barton GJ. 2009. Jalview Version 2--
525 a multiple sequence alignment editor and analysis workbench. *Bioinformatics* 25:1189-
526 91.

527 40. Johnson CJ, Nett JE. 2022. Examining Neutrophil-*Candida auris* Interactions with
528 Human Neutrophils Ex Vivo. *Methods Mol Biol* 2517:243-250.

529

530

531 Table 1. Strains used in this study.

Strain	Parent	Genotype
SN152	SC5314	<i>arg4Δ/arg4Δ leu2Δ/leuΔ his1Δ/his1Δ URA3/ura3Δ::imm</i> <i>IRO1/iro1Δ::imm</i>
LLF100	SN152	(<i>Prototrophic wild-type control</i>) <i>ARG4/arg4Δ LEU2/leu2Δ</i> <i>HIS1/his1Δ URA3/ura3Δ::imm IRO1/iro1Δ::imm</i>
LLF054	SN152	<i>pst3-ycp4Δ::HIS1/pst3-ycp4Δ::LEU2</i> <i>pst2Δ::frt/pst2Δ::frt</i> <i>pst1Δ::frt/pst1Δ::frt arg4Δ /arg4Δ</i>
LLF060	LLF054	($\Delta/\Delta/\Delta/\Delta$) <i>pst3-ycp4Δ::HIS1/pst3-ycp4Δ::LEU2</i> <i>pst2Δ::frt/pst2Δ::frt pst1Δ::frt/pst1Δ::frt ARG4/arg4Δ</i>
<i>zta1Δ/Δ</i>	SN152	<i>zta1Δ::HIS1/zta1Δ::HIS1 ARG4/arg4Δ LEU2/leu2Δ</i> <i>URA3/ura3Δ::imm IRO1/iro1Δ::imm</i>
<i>zta1+</i>	SN152	($+ZTA1$) <i>zta1Δ::HIS1/zta1Δ::HIS1 ZTA1::NAT1::NEUT5L</i> <i>ARG4/arg4Δ LEU2/leu2Δ URA3/ura3Δ::imm IRO1/iro1Δ::imm</i>
Q Mut	LLF054	<i>pst3-ycp4Δ::HIS1/pst3-ycp4Δ::LEU2</i> <i>pst2Δ::frt/pst2Δ::frt</i> <i>pst1Δ::frt/pst1Δ::frt ARG4/arg4Δ</i>
Q Mut+	LLF054	($+ZTA1$) <i>zta1Δ::HIS1/zta1Δ::HIS1 ZTA1::NAT1::NEUT5L</i> <i>pst3-ycp4Δ::HIS1/pst3-ycp4Δ::LEU2</i> <i>pst2Δ::frt/pst2Δ::frt</i> <i>pst1Δ::frt/pst1Δ::frt ARG4/arg4Δ</i>

532

533

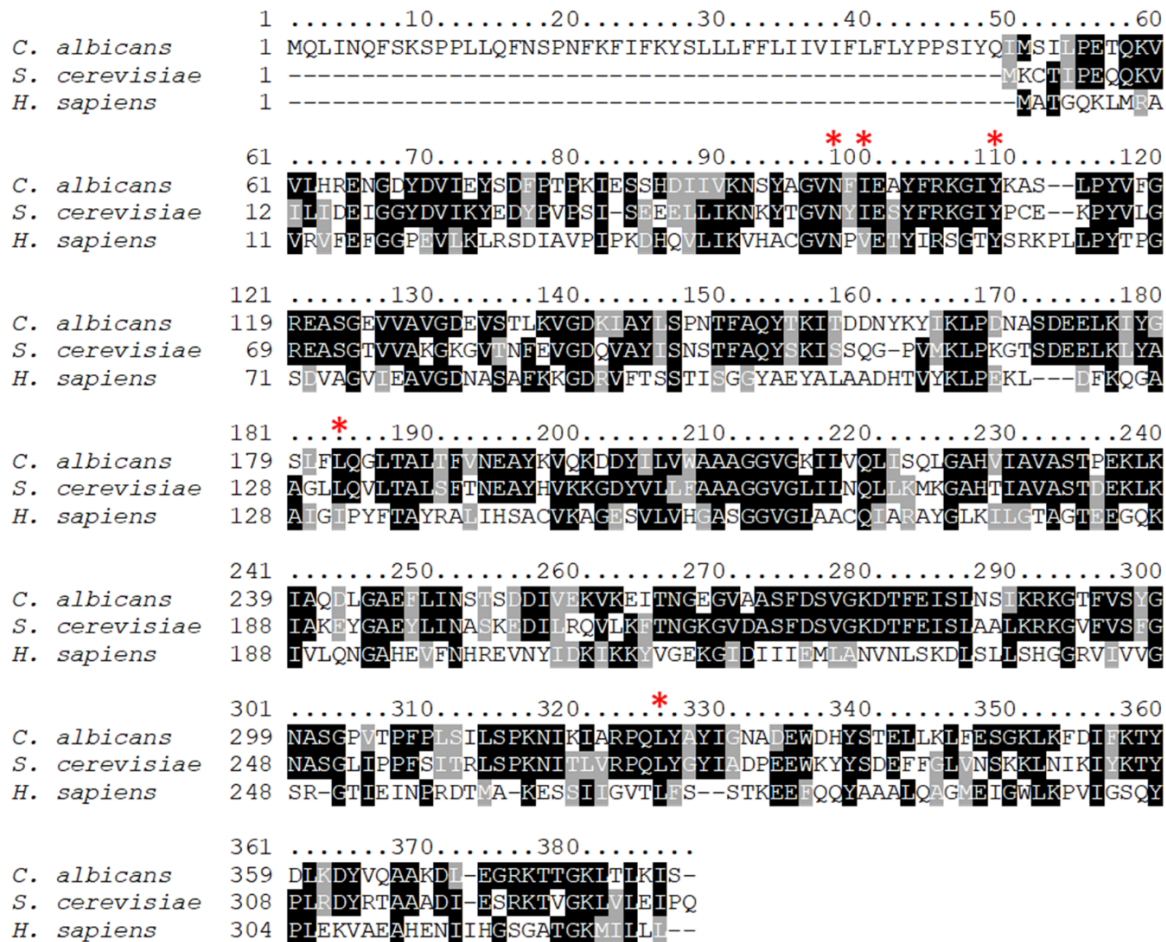
534

Table 2. Primers used in this study

Primer name	Sequence
GFPFwD1	ACGATTGAAAGATTACGTTCAAGCTGCAAAGATTGGAAGGCAGAAAAACTACT GGTAAGTTAACATTAACATTTCTGGTGCAGGTGCTTC
GFPFwD2	TCCTCAAGATTGATGAAGTACGAACAGTCAGACCTAAATTATAATTACATAAATA TTCAATAATACATGAACATCTGATATCATCGATGAATTGAG
Zta1HisDel1	TGTTTTTTTATTGGTAGCGAAGTCTATAAGAACAAACGGAAAACCACAGTTTT TTTCTCTCTCGCATAGTGAATATGCTCGGATCCACTAGTAACG
Zta1HisDel2	TACTCCTCAAGATTGATGAAGTACGAACAGTCAGACCTAAATTATAATTACATAA ATATTCAATAATACATGAACATAATGCTCGAGCGGCCAGTG
SNR52R	CCCACTACTTCAGTTCAATTCAAATTAAAAAGTTACCGCAAGTC
SgRNAF	AATTGAACTGAAGTAGTGGGTTTAGAGCTAGAAATAGCAAGTTAA
3118	CCAGATGCGAAGTTAAGTGGCAG
4926	AAAAGGCCTGATAAGGAGAGATCCATTAAGAGCA
5227	GGTCATAGCTGTTCTGTGAAATTGTTATCCGCTCACTGGATACGGATTCT TACG
5228	GGCCCCCCTCGAGGTCGACGGTATCGATAAGCTTGATATCTCAAATAGAACTG CTCCC

535

536



537

538

Fig 1. Conservation of Zta1 protein sequence.

539

540

540

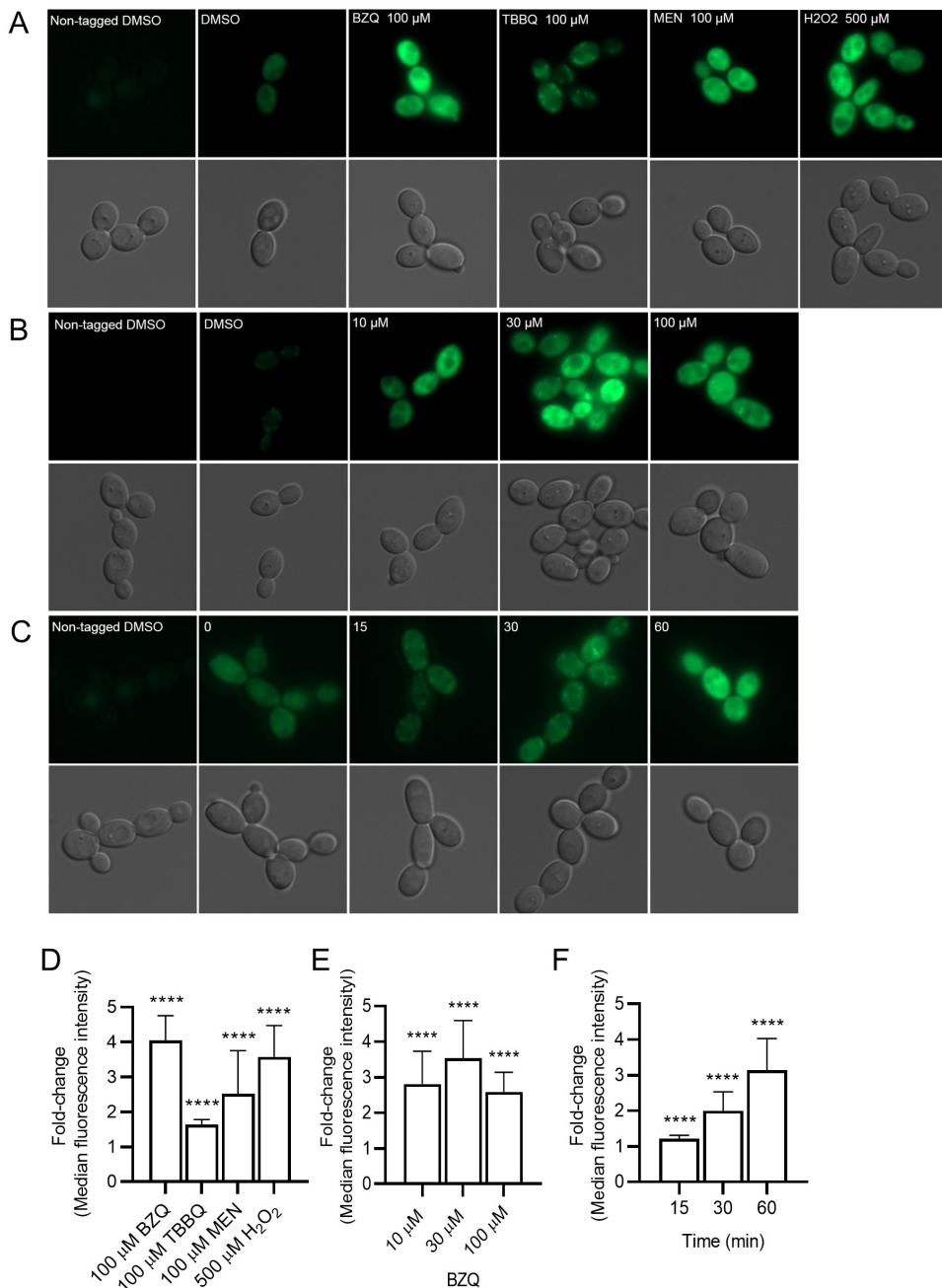
541

542

543

24

544

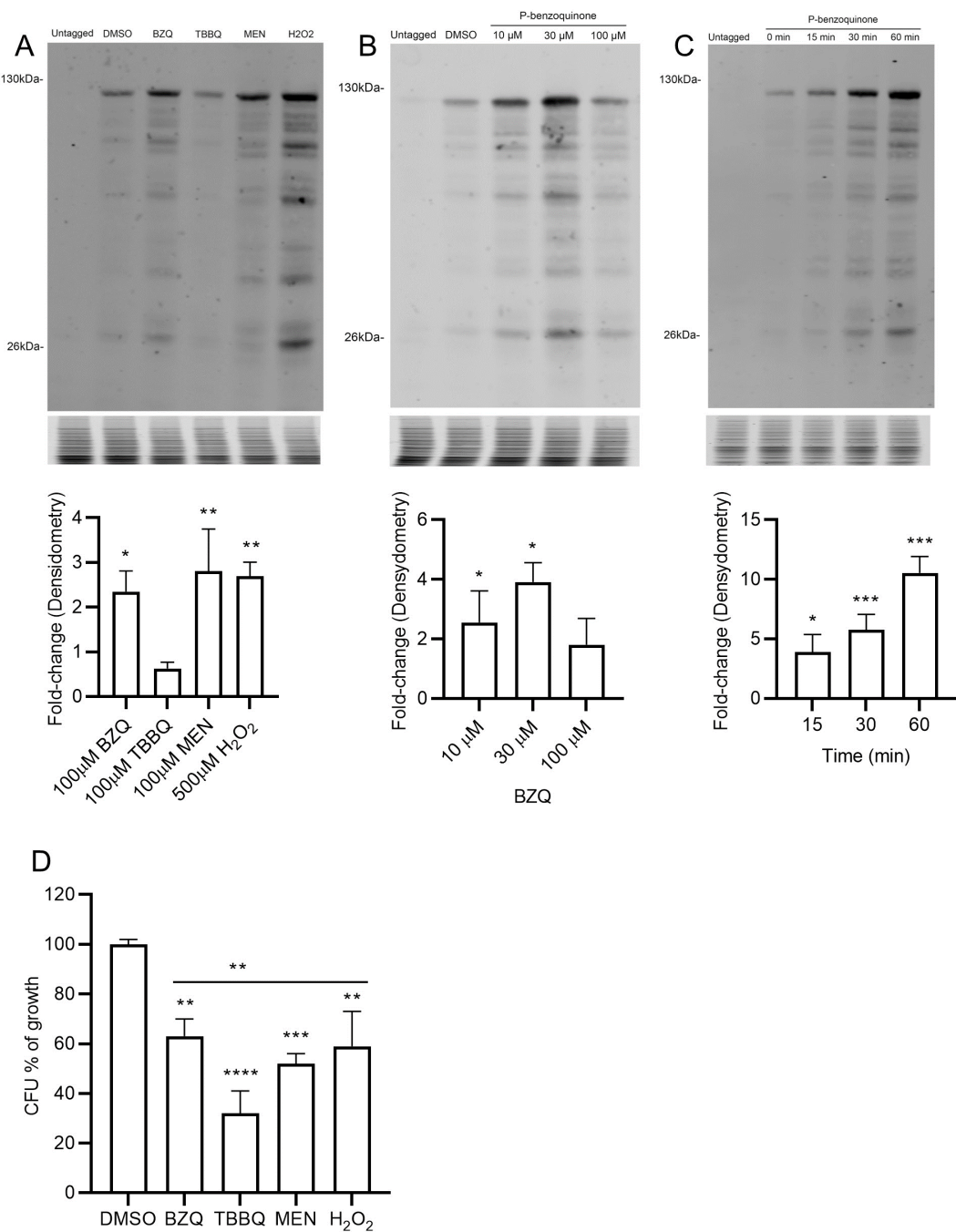


545
546

547 **Fig. 2** Fluorescence microscopy of *C. albicans* cells producing Zta1.
548 (A) *C. albicans* ZTA1-3xGFP cells were incubated with 100 µM of p-benzoquinone (BZQ), 2-tert-
549 butyl-1,4-benzoquinone (TBBQ), Menadione (MEN) and 500 µM of hydrogen peroxide (H₂O₂) at
550 30°C for 1 h, washed and then imaged by fluorescence microscopy.
551 (B) *C. albicans* ZTA1-3xGFP cells were treated with different concentrations of p-benzoquinone
552 (10, 30 and 100 µM) for 1 h and then analyzed.

553 (C) cells were treated with 100 μ M of p-benzoquinone and imaged after the indicate minutes of
554 incubation.
555 (D-F) Median fluorescence intensity of *ZTA1-3xGFP* cells treated with
556 (D) the indicated compounds for 1 h,
557 (E) different concentrations of p-benzoquinone for 1 h and
558 (F) 100 μ M p-benzoquinone for the indicated times. The bars represent the average fold-change
559 of 3 independent assays performed on different days. *t* tests were performed comparing each
560 condition to the control cells treated with DMSO. ****, $P \leq 0.0001$.
561

562



563

564

Fig. 3 Zta1 is induced by quinones and oxidation.

565

566

567

568

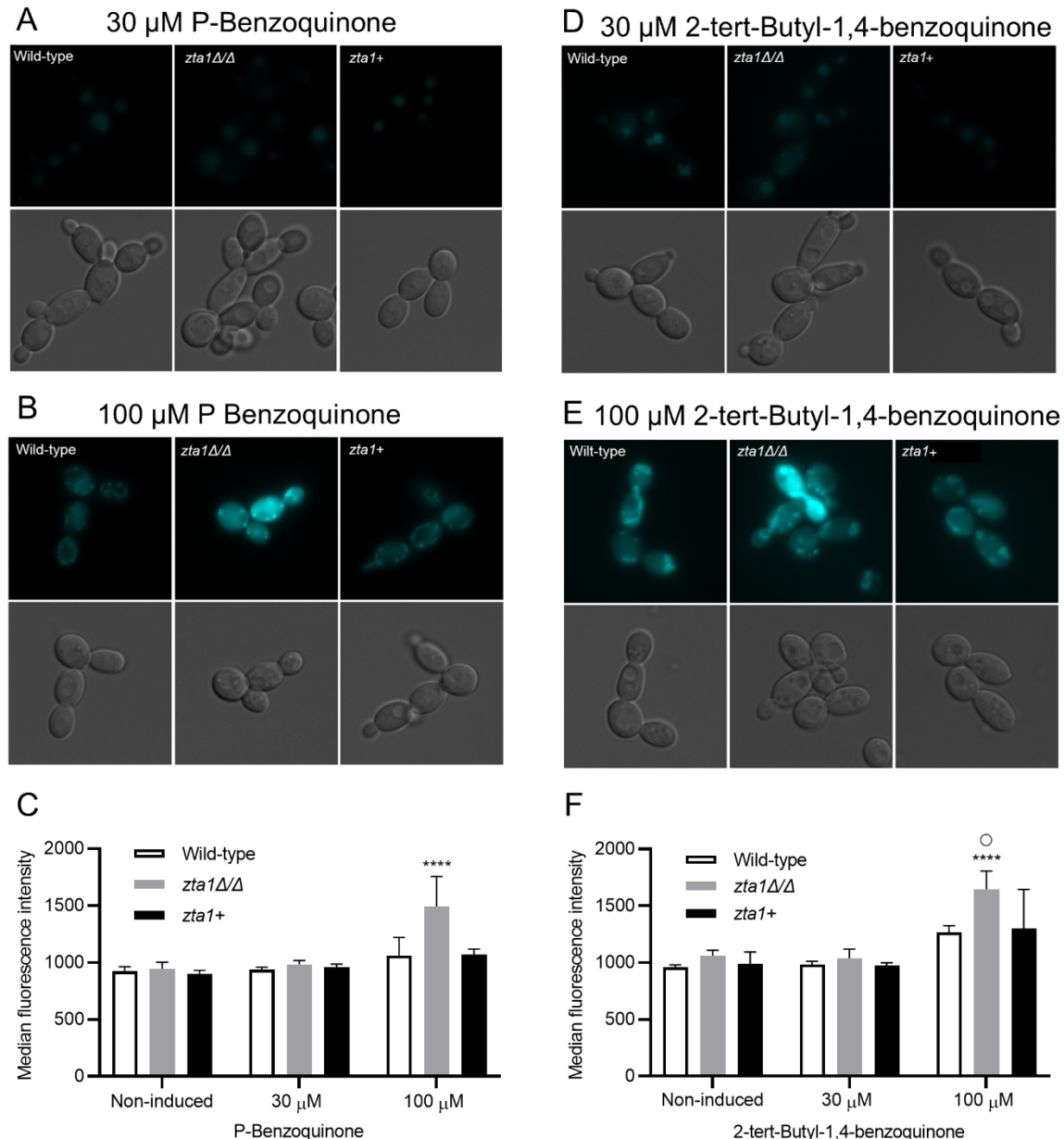
569

570

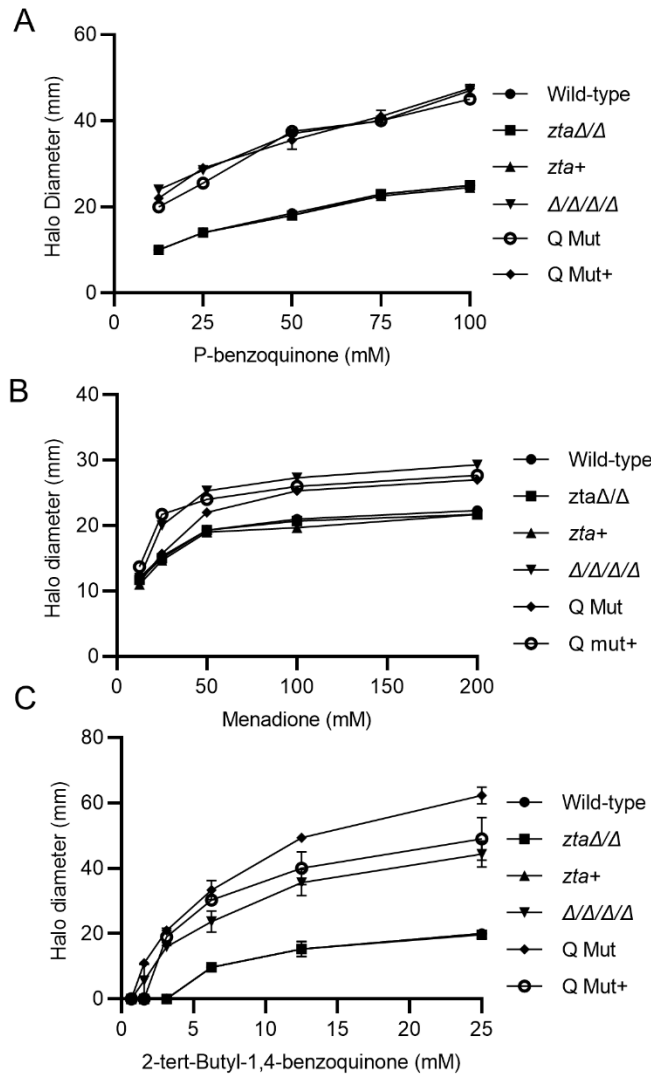
571

Western blots comparing Zta1-3xGFP production in *C. albicans* exposed to (A) the indicated oxidants for 1 h, (B) different concentrations of p-benzoquinone for 1 h, or (C) 100 μM of p-benzoquinone for the indicated times. Cells exposed to DMSO were used as a control. Western blots probed with anti GFP antibodies are shown on the top, Coomassie Blue stained gels of the protein samples shown below were used as a loading control. The bar graphs underneath showing quantitation of the results was performed using Image Studio

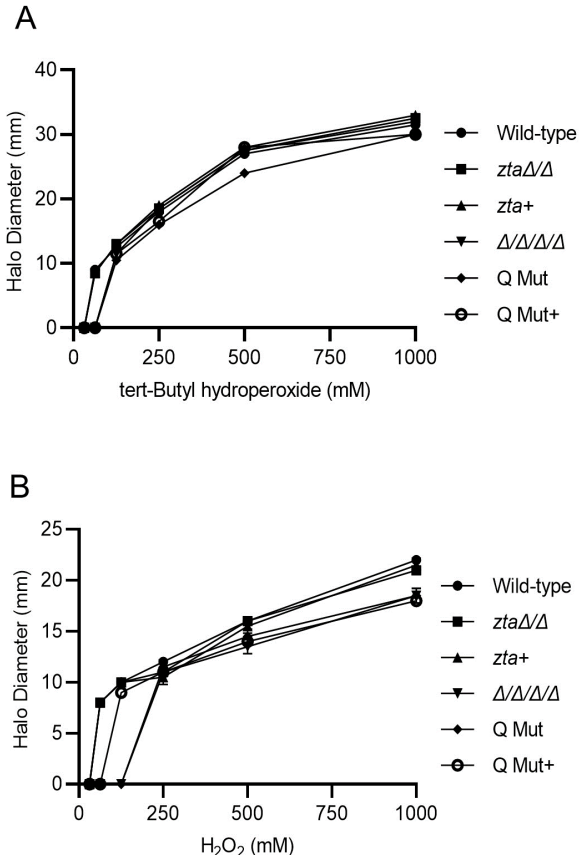
572 software, normalized to Coomassie-stained gels. The results represent the average of three
573 independent experiments performed on different days.
574 (D) CFU assay of Zta1-3xGFP tagged cells treated with 100 μ M of BZQ, TBBQ, MEN and 500
575 μ M of H_2O_2 for 1 h.
576 Results represent averages from three independent experiments performed on different days.
577 Multiple *t* tests were performed comparing each condition to the DMSO-treated control. **,
578 $P \leq 0.01$; ***, $P \leq 0.001$, **** $P \leq 0.0001$. *t* tests were also performed comparing TBBQ with the
579 other conditions, **, $P \leq 0.01$.
580
581



582
583 **Fig. 4.** ROS accumulation is higher in the $zta1\Delta/\Delta$ mutant exposed to quinones.
584 Wild-type, $zta1\Delta/\Delta$ and $zta1^+$ complemented strains were exposed to (A) 30 μ M or (B) 100 μ M
585 p-benzoquinone, or (D) 30 μ M or (E) 100 μ M 2-tert-butyl-1,4-benzoquinone for 1h and then the
586 accumulation of reactive oxygen species was assayed by incubating the cells with 2',7'-
587 Dichlorofluorescein diacetate for 20 min before imaging by fluorescence microscopy.
588 (C) Median fluorescence intensity for panels A and B.
589 (F) Median fluorescence intensity for panels D and E.
590 Bars represent the average median fluorescence intensity of 3 independent assays on different
591 days. ****, $P \leq 0.0001$, by one-way analysis of variance (ANOVA). ○, $P \leq 0.05$, by t-test (100 μ M
592 of p-benzoquinone vs. 100 μ M 2-tert-butyl-1,4-benzoquinone) The wild type control strain was
593 LLF100. The strains are described in Table 1.
594



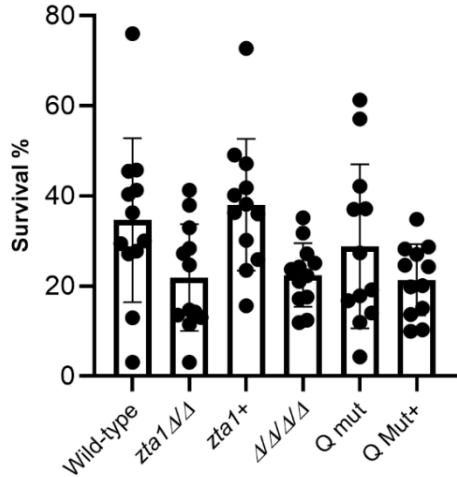
595
596 **Fig. 5.** Zta1 acts in combination with FLPs to promote resistance to 2-tert-butyl-1,4-
597 benzoquinone.
598 Quantification of disk diffusion halo assays comparing the susceptibility of *C. albicans* strains to
599 (A) p-benzoquinone, (B) menadione and (C) 2-tert-butyl-1,4-benzoquinone. The x-axis indicates
600 the concentration of the compound applied to the disk and the y-axis indicates the diameter of
601 the zone of growth inhibition. The strains tested included the wild-type control strain (LLF100),
602 *zta1Δ/Δ*, *zta1+*, $\Delta/\Delta/\Delta/\Delta$, Q Mut, and Q Mut+ complemented strain (see Table 1). Results
603 represent the averages from at least three independent experiments, each done in duplicate.
604 Error bars indicate SD.
605



606
607
608
609
610
611
612
613
614

Fig.6 The $zta1\Delta/\Delta$ mutant does not show increased susceptibility to peroxides.

Quantification of disk diffusion halo assays comparing the susceptibility of *C. albicans* strains to tert-butyl-hydroperoxide and hydrogen peroxide (H_2O_2). The strains tested included the wild-type control strain (LLF100), $zta1\Delta/\Delta$, zta^+ , $\Delta/\Delta/\Delta/\Delta$, Q Mut, and Q Mut+ complemented strain (see Table 1). Results represent the averages from at least three independent experiments, each done in duplicate. Error bars indicate SD.

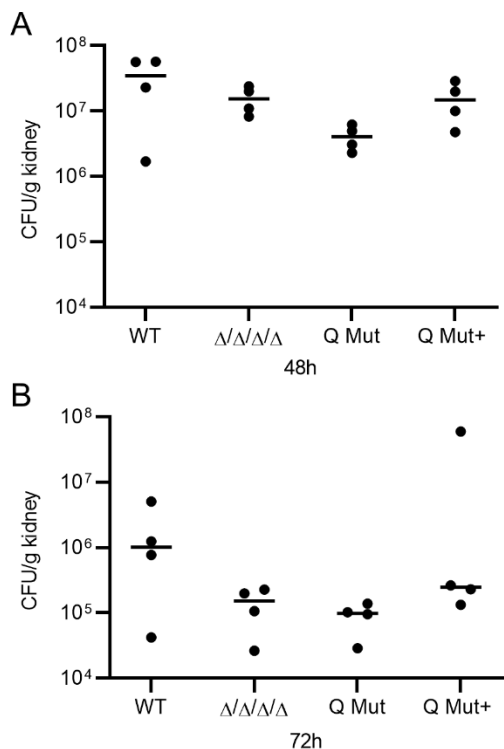


623
624
625
626
627
628
629
630

Fig. 7 Susceptibility of *C. albicans* strains to attack by human neutrophils.

Human neutrophils from 4 different donors were incubated with the wild-type control strain (LLF100), *zta1Δ/Δ*, *zta1+*, FLP mutant ($\Delta/\Delta/\Delta/\Delta$), Q Mut and Q Mut+ (complemented with *zta1*) during 4 h. Yeast viability and percentage of survival was determined using PrestoBlue dye. Data are presented as the mean of four independent experiments, each done in triplicate. Error bars indicate SD. Strains are described in Table 1.

631



632

633

634 **Fig. 8** Zta1 role in *C. albicans* virulence.

635 Female Balb/c mice were infected with 2.5×10^5 cells of the indicated *C. albicans* strain via the
636 tail vein. Strains used included the LLF100 wild-type control strain, FLP mutant ($\Delta/\Delta/\Delta/\Delta$), Q Mut
637 and Q Mut+ (complemented with *zta1*) (see Table 1). CFU/g of kidney was determined at (A)
638 day 2 and (B) day 3 post infection. Four mice were injected with each strain for each day of
639 analysis and their mean is presented.